ELSEVIER

Journal of Chromatography A, 845 (1999) 103–111

JOURNAL OF CHROMATOGRAPHY A

Measurement of adsorption energies on heterogeneous surfaces by inverse gas chromatography

Nicholas A. Katsanos[a,*], Nicholaus Rakintzis[b], Fani Roubani-Kalantzopoulou[b], Evagelia Arvanitopoulou[a], Athanasios Kalantzopoulos[b]

[a]*Physical Chemistry Laboratory, University of Patras, 26500 Patras, Greece*

[b]*Department of Chemical Engineering, National Technical University of Athens, 15780 Zografou, Greece*

Abstract

Inverse gas chromatography methods, like the reversed-flow gas chromatography technique, offer a new pathway to the determination of adsorption energies of gaseous substances on heterogeneous solid adsorbents, as a function of time. The theoretical development was based on the local isotherm model of Jovanovic, and the experimental arrangement was a simple gas chromatograph, slightly modified. The method was applied to four gas–solid systems, at 323.2 K, namely, gaseous C_2H_4 and ZnO, PbO, TiO_2, Fe_2O_3, the solids also being γ-irradiated with 8.2 Mrad before adsorption experiments. The results obtained point to the conclusion that a time transition period with respect to the adsorption energy exists, consisting of maxima and minima in the values of energy with time. It ends by levelling off at long times. The kinetic physicochemical quantities of adsorption have also been measured.

Keywords: Inverse gas chromatography; Adsorption energy

1. Introduction

Dynamic measurements by means of gas adsorption chromatography (GSC) have become a popular and powerful method of investigating adsorption phenomena, since they are fast and simple, and commercially available equipment makes increasingly precise measurements possible. The majority of physicochemical adsorption properties studied by GSC refers to the stationary phase and its interaction with known probe solutes, and this is known as inverse gas chromatography, since it has the stationary phase of the system as the main object of investigation. Usually, the same procedures as in direct GSC are employed, the results being used to derive, among others, adsorption properties of the stationary phase. Adsorption energies on heterogeneous surfaces is an important property, their main method of determination being the measurement of net retention volumes V_N at various temperatures T and the plotting of $\ln V_N$ against $1/T$:

$$\ln V_N = \ln (RTn_s) + \frac{\Delta S}{R} - \frac{\Delta H}{R} \cdot \frac{1}{T} \quad (1)$$

where R is the gas constant, n_s (mol) the total amount of the solute in the adsorbed state and ΔH, ΔS the differential enthalpy and differential entropy of adsorption, respectively [1]. The calculation of acceptable values for ΔH and ΔS requires that the range of T is narrow enough. An analogous way for calculating differential enthalpy and entropy of adsorption by GSC has been described by Milonjic and

*Corresponding author. Tel.: +30-61-997-110; fax: +30-61-997-110.

E-mail address: Katsanos@otenet.gr (N.A. Katsanos)

0021-9673/99/$ – see front matter
PII: S0021-9673(99)00262-9

Copecni [2]. The isosteric enthalpy of adsorption ΔH_{st} is simply found by the relation $\Delta H_{st} = \Delta H + RT$.

The above, including analysis by statistical mechanics, were recently reviewed [3], but it has to be pointed out that such classical gas chromatography (GC) systems are not in true equilibrium during the retention period, needing extrapolation to infinite dilution and zero carrier gas flow-rate, to approximate true equilibrium. Inverse GSC was also employed for characterizing heterogeneous solids by calculating adsorption energy distribution functions from retention volume data [3], but not adsorption energy values.

An inverse gas chromatographic tool is the reversed-flow (RF) GC technique for physicochemical measurements, which dismisses the carrier gas from doing the work, and ''appoints'' the gaseous diffusion process in its place. The carrier gas performs only the sampling procedure to measure the gas-phase concentration of an analyte A at a certain position as a function of time. The RF-GC technique has been used for measurement of various physicochemical quantities [3], to mention only the simultaneous determination of six parameters pertaining to the deposition of air pollutants on solid surfaces, including rate constants of surface and gaseous reactions, and experimental isotherms [4]. The only physicochemical assumptions concerning the gas–solid interactions are that all parameters measured directly or calculated indirectly refer to elementary steps at equilibrium. Based on that, the ratio of the rate constant for adsorption to that of desorption, both determined experimentally [3,4], is an equilibrium distribution constant, according to the principle of microscopic reversibility. It is not an easy thing to measure simultaneously rate constants of adsorption and desorption at a dynamic equilibrium state like that justified experimentally in the RF-GC technique. It seems that RF-GC offers a new pathway to the determination of adsorption energy values of gaseous substances on heterogeneous solid surfaces, as distributed over the instrumental time, i.e., time measured from the moment of introduction of the gas under study into the solid bed, and continued as long as the chromatographic detector records substance concentrations. The method is described in the present paper and exemplified by presenting representative results.

2. Theory

In order to find the adsorption energy ε responsible for the observed local isotherm $\theta(p, T, \varepsilon)$, not statically but dynamically as a function of time, only a local (homogeneous) isotherm model is required and a fairly general one for our purposes is that of Jovanovic [5]:

$$\theta(p, T, \varepsilon) = 1 - \exp(-Kp) \tag{2}$$

going over to Langmuir isotherm in middle pressures, and to a linear form at low pressures. The K is Langmuir's constant given by the relation [6]

$$K = K^0(T)\exp(\varepsilon/RT) \tag{3}$$

where R is the gas constant, and $K^0(T)$ is described by statistical mechanics [7], as

$$K^0 = \frac{h^3}{(2\pi m)^{3/2}(kT)^{5/2}} \cdot \frac{v_s(T)}{b_g(T)} \tag{4}$$

k being the Boltzmann constant, m the molecular mass, h the Planck constant, $b_g(T)$ the partition function for the rotations and vibrations of the free gas molecule and $v_s(T)$ the partition function of the adsorbed molecule over all possible quantum states. As a low temperature approximation, we adopt that $v_s(T) \approx b_g(T)$, as was done before [6].

Although the physical foundations of Eq. 2 have been criticized [8], this isotherm gives a good representation of experimental gas adsorption and behaves correctly at a wide range of surface coverages. An exhaustive numerical investigation of the differences in the behavior of the Jovanovic isotherm compared with that of Langmuir [9] led to the conclusion that, for the system krypton–pyrex, there is nothing to choose between the two and both give very similar values of the monolayer capacities. Also, Sircar [10] used the Jovanovic isotherm as the kernel $\theta(\varepsilon, T, p)$ in the well-known integral equation of the energy distribution function $f(\varepsilon)$:

$$v(p, T) = \int_0^\infty \theta(\varepsilon, T, p) f(\varepsilon) \mathrm{d}\varepsilon \tag{5}$$

where $v(p, T)$ is the adsorbed amount, and showed that Eq. 5 takes a simple compact form and results in an energy distribution function of the same form

with that obtained by using the Langmuir isotherm as the kernel. Only the variance of the calculated function is affected. Jaroniec et al. [11] investigated the possibility of extending the Jovanovic equation to multilayer adsorption on heterogeneous surfaces. In discussing numerical methods of evaluating the adsorption energy distribution from Eq. 5, Rudzinski and Everett [12] describe the application of Laplace transforms to Jovanovic equation used as the local adsorption isotherm $\theta(p, T, \varepsilon)$, not only to monolayer but also to multilayer adsorption. They point out that the Jovanovic equation yields a remarkably different picture of surface heterogeneities. For example, three distinct kinds of adsorption sites for the system argon–rutile appear in the distribution based on the Jovanovic model, whereas the Langmuir model shows signs of three peaks, but the two of them are barely distinguishable. Landman and Montroll [13] investigated the energy distribution function which converts the Langmuir local isotherm into the Jovanovic equation. The temperature dependence of this function shows that the picture of surface heterogeneity given by the Jovanovic and the Langmuir isotherms becomes more and more different as temperature increases.

The short review above regarding the Jovanovic isotherm (Eq. 2) justifies its use in the present work to calculate adsorption energies of gases on solids by inverse GSC in the form of RF-GC. The experimental arrangement, on which the following theoretical analysis is based, has been published before [4] and is repeated in Fig. 1 for convenience. Injecting a small amount of the adsorbate gas or vapor A (0.5–1 cm^3 under atmospheric pressure) at the end $y=L_2$ of the solid bed, and making repeated flow-reversals of short duration (10–60 s) of the carrier gas (air or N_2) by means of the four-port valve, one obtains in the recorder a series of narrow, symmetrical *sample peaks* of considerable height H above the continuous chromatographic signal, depending on the time t at which the flow reversal was made.

A mathematical model [3,4] based on two mass balances of the analyte A (in the regions z and y of the diffusion column), together with the rate of change of the adsorbed concentration c_s (mol/g) and a local experimental isotherm for the equilibrium concentration c^*_s (mol/g) at time t, leads to the following function $H=f(t)$:

$$H^{1/M} = \sum_{i=1}^{4} A_i \exp(B_i t) \tag{6}$$

where M is the response factor of the detector. The coefficients of time B_i, calculated by non-linear regression analysis with a PC program in GW-BASIC [3,4] from the experimental pairs H, t, lead to the calculation of various physicochemical quantities among which are the adsorption and desorption

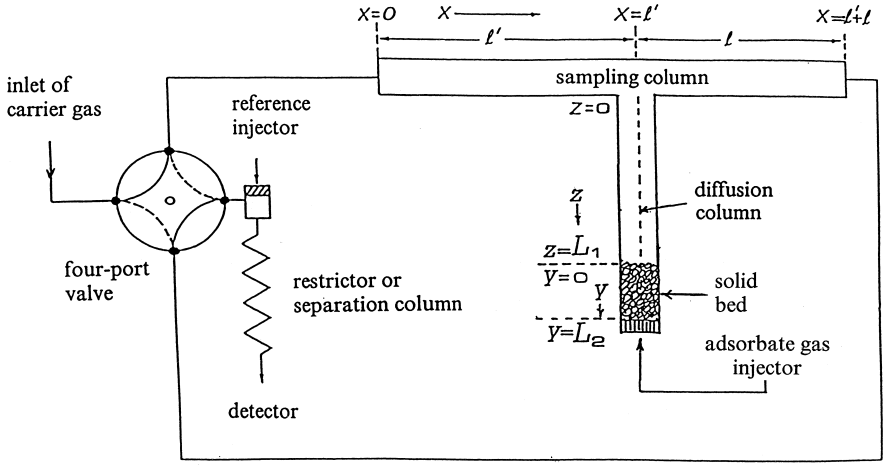

Fig. 1. Schematic representation of columns and gas connections for the use of the reversed-flow technique as an inverse gas chromatography tool.

rate constants k_1 (s^{-1}) and k_{-1} (s^{-1}), respectively, of the adsorbate A on the heterogeneous surface, and the gaseous concentration of A above the solid c_y (mol cm^{-3}), at $y=0$ of the solid bed (cf. Fig. 1):

$$c_y = \frac{vL_1}{gD_1}\sum_{i=1}^{4} A_i \exp(B_i t) \tag{7}$$

where g is the calibration factor of the chromatographic detector [14] in cm (peak height)/mol cm^{-3}, D_1 the diffusion coefficient of A into the carrier gas, v the corrected linear flow velocity of the carrier gas and L_1 the length of section z of the diffusion column.

The fraction of the surface covered at time t is denoted as $\theta_t = c^*_s/c^*_{max}$, c^*_{max} being the local (homogeneous) monolayer capacity, i.e., the maximum adsorbed concentration of the gaseous substance A at time t. Instead of the partial pressure of A, p, we write c_yRT, considering A as ideal gas. Therefore, according to Eq. 2

$$\theta_t = \frac{c^*_s}{c^*_{max}} = 1 - \exp(-KRTc_y) \tag{8}$$

From this, one can calculate the first two derivatives of θ_t with respect to c_y, keeping in mind that c^*_{max} is a constant for each kind of active sites. By division of the two above derivatives, one obtains

$$-\frac{\partial^2 c^*_s}{\partial c_y^2}\Big/\frac{\partial c^*_s}{\partial c_y} = KRT = RTK^0 \exp(\varepsilon/RT) \tag{9}$$

Thus, the calculation of the two derivatives $\partial c^*_s/\partial c_y$ and $\partial^2 c^*_s/\partial c_y{}^2$ from experimental data leads directly to the value of ε for the kind of sites i being responsible for the adsorption at time t, since everything else on the right-hand side of Eq. 9 is known. The general experimental function of time (Eq. 6) of the RF-GC method permits an easy and accurate way to calculate $\partial c^*_s/\partial c_y$ and $\partial^2 c^*_s/\partial c_y^2$ from experimental data. The first derivative, as already published [14], is

$$\frac{\partial c^*_s}{\partial c_y} = \frac{a_y}{a_s}\cdot k_1 \cdot \frac{\sum_{i=1}^{4} A_i \exp(B_i t)}{\sum_{i=1}^{4} A_i B_i \exp(B_i t)} \tag{10}$$

where a_y is the cross sectional area of the void space in the solid bed, and a_s the amount of solid per unit length of bed (g/cm). The second derivative $\partial^2 c^*_s/\partial c_y{}^2$ is found from Eq. 6 as a function of time t as follows:

$$\frac{\partial^2 c^*_s}{\partial c_y^2} = \frac{\partial^2 c^*_s}{\partial c_y \partial t}\Big/\frac{\partial c_y}{\partial t} \tag{11}$$

The second mixed derivative of the numerator on the right-hand side is simply obtained from Eq. 10 by differentiating with respect to time t:

$$\frac{\partial^2 c^*_s}{\partial c_y \partial t} = \frac{a_y}{a_s}\cdot k_1 \cdot\left\{1 - \frac{\left[\sum_i A_i \exp(B_i t)\right]\left[\sum_i A_i B_i^2 \exp(B_i t)\right]}{\left[\sum_i A_i B_i \exp(B_i t)\right]^2}\right\} \tag{12}$$

The denominator of Eq. 11 is obtained by differentiating Eq. 7 with respect to time t:

$$\frac{\partial c_y}{\partial t} = \frac{vL_1}{gD_1}\sum_i A_i B_i \exp(B_i t) \tag{13}$$

Division of Eq. 12 by Eq. 13, according to Eq. 11, gives the desired second derivative:

$$\frac{\partial^2 c^*_s}{\partial c_y^2} = \frac{a_y}{a_s}\cdot k_1 \cdot\frac{gD_1}{vL_1}\left\{\frac{1}{\sum_i A_i B_i \exp(B_i t)} - \frac{\left[\sum_i A_i \exp(B_i t)\right]\left[\sum_i A_i B_i^2 \exp(B_i t)\right]}{\left[\sum_i A_i B_i \exp(B_i t)\right]^3}\right\} \tag{14}$$

Using Eqs. 10 and 14 in Eq. 9, one calculates as a function of time KRT and from this the value of ε at

any chosen time t of the experiment:

$$KRT = \frac{gD_1}{vL_1}\left\{\frac{\left[\sum_i A_i B_i^2 \exp(B_i t)\right]}{\left[\sum_i A_i B_i \exp(B_i t)\right]^2} - \frac{1}{\sum_i A_i \exp(B_i t)}\right\} \quad (15)$$

$$\varepsilon = RT\left[\ln(KRT) - \ln(RT) - \ln K^0\right] \quad (16)$$

3. Calculations

The calculation of the adsorption energy on heterogeneous surfaces starts from the diffusion band of RF-GC experiments, comprising the values of the pairs H, t. From these, the time coefficients B_1, B_2, B_3 and B_4 of Eq. 6 are extracted, together with the rate constants k_1, k_{-1} and k_2, the calibration factor g and the diffusion coefficient D_1 of the gaseous analyte into the carrier gas, by means of a personal computer (PC) program published in the Appendix of Ref. [3]. The other quantities needed v, L_1, R, k, h, T and m are known from literature or from conventional measurements. The values of D_1 calculated by the PC program represent an effective diffusion coefficient owing to the obstruction factor γ of the solid bed, arising from the tortuosity of the paths through the bed and the alternating constriction and widening of these paths. Introducing all above quantities into another simple PC program based on Eq. 4 for K^0, on Eq. 15 for KRT and finally on Eq. 16, one finds the value of ε in the simplest possible way and for several times (within the frame of the experimental time t). The c_y value corresponding to these values can simply be calculated by means of Eq. 7.

Instead of the above procedure, one may use a compact PC program in GW-BASIC obtainable from the corresponding author (N.A.K.) to calculate directly from the experimental pairs H, t the values of ε and c_y, together with the adsorption parameter k_1, the desorption rate constant k_{-1}, a possible first-order surface reaction rate constant k_2, the effective diffusion coefficient D_1 of the probe gas into the carrier gas, and the calibration factor of the detector g. The values M in Eq. 6, v and L_1 needed in Eqs. 7 and 15, and some other known data are entered into the appropriate INPUT lines of the above program, together with the range of times t_1 and t_2 in which ε and c_y are calculated and printed. A step of 2 min is arbitrarily set in the program, but this can be changed to smaller distances between calculation times, or Eqs. 7 and 16 may be used with the PC program MATHEMATICA 3 to plot ε and c_y vs. t between the two limits of the experimental time with a number of plot points say 3000.

4. Experimental

The chromatographic apparatus was a Shimadzu 8A gas chromatograph equipped with a flame ionization detection (FID) system. The cell of Fig. 1 had the following dimensions. The empty diffusion column L_1 had a length of 20.5–23.5 cm, whereas section L_2 (filled with the solid) was 2.8–5.0 cm long. Both were constructed from pyrex glass of I.D. 3.5 mm. The sampling column $l'+l$ (40+40 cm) was a stainless steel chromatographic tube of I.D. 4 mm. No separation column was employed, and the whole cell was accommodated inside the oven of the chromatograph and heated at a constant temperature.

The carrier gas was pure nitrogen for chromatographic analysis, with a flow-rate of 26.1 cm^3/min. It was obtained from Air Liquide (Athens, Greece), together with ethene. Both gases had a purity of better than 99.5%.

The solid adsorbents (ZnO, PbO, TiO_2 and Fe_2O_3) were pro-analysi products of Merck. In one series of experiments a conditioning of the solid bed was carried out in situ, at 473.2 K for 24 h, under a continuous carrier gas flow. After cooling at the working temperature of 323.2 K, the whole series of the sample peaks was obtained by the procedure described elsewhere [4], by injecting 1 cm^3 of ethene at atmospheric pressure through the injector at $y=L_2$ (cf. Fig. 1), and repeatedly reversing the carrier gas-flow for 10 s by means of the four-port valve.

In a second series of experiments, the solid bed, after the conditioning described above, was irradiated with γ rays from Co-60 for 27 h and 20 min with a dose of 5000 rad/min, i.e., a total dose of 8.2

Mrad. After irradiation, the samples of the four solids were placed in the chromatograph and used as before without a new conditioning.

By entering the pair of values of H, t into the DATA lines of the GW-BASIC program obtainable by writing to N.A.K., together with the other known quantities in the relevant INPUT lines, all physicochemical quantities k_1, k_{-1}, k_2, D_1, g, ε and c_y, defined in the Section 2 were calculated and printed.

5. Results and discussion

The method described in the present work to measure directly the adsorption energies as a function of the experimental time was applied to gaseous ethene being adsorbed on four solid adsorbents, namely, ZnO, PbO, TiO_2 and Fe_2O_3, before and after γ-irradiation with a dose of 8.2 Mrad. Tables 1 and 2 list the values of the adsorption energies for a

Table 1
Time distribution of gaseous concentration (c_y) for C_2H_4 and its adsorption energy (ε) on ZnO and PbO solids, before and after γ-irradiation with 8.2 Mrad, at 323.2 K

Time (min)	c_y ($\cdot 10^{-6}$ mol/cm^3)		ε (kJ/mol)		c_y ($\cdot 10^{-6}$ mol/cm^3)		ε (kJ/mol)	
	ZnO	ZnO (irrad.)	ZnO	ZnO (irrad.)	PbO	PbO (irrad.)	PbO	PbO (irrad.)
4	4.95	5.44	87.1	86.3	3.20	7.52	87.9	86.7
6	6.80	8.16	88.3	86.7	4.65	9.93	88.4	87.8
8	7.71	9.73	90.9	88.1	5.48	11.0	89.7	89.5
10	8.05	10.6	96.6	90.3	5.94	11.6	91.7	92.4
12	8.06	10.9	97.1	94.5	6.16	11.7	95.0	100.5
14	7.88	11.0	91.0	104.5	6.23	11.7	106.2	95.6
16	7.60	10.9	88.1	93.0	6.20	11.5	96.6	90.9
18	7.27	10.7	86.0	89.6	6.11	11.2	92.4	88.4
20	6.93	10.4	84.3	87.5	5.98	10.9	90.1	86.7
22	6.57	10.1	82.7	85.9	5.82	10.5	88.5	85.4
24	6.23	9.72	81.0	84.6	5.64	10.1	87.2	84.4
26	5.90	9.36	78.9	83.5	5.45	9.64	86.2	83.4
28	5.59	8.99	75.3	82.5	5.26	9.21	85.4	82.5
30	5.29	8.63	74.6	81.6	5.07	8.78	84.6	81.7
32	5.01	8.27	77.0	80.8	4.88	8.36	84.0	80.8
34	4.74	7.93	77.8	79.9	4.69	7.96	83.3	80.0
36	4.49	7.59	78.1	79.0	4.50	7.57	82.7	79.0
38	4.25	7.27	78.2	78.1	4.32	7.20	82.1	77.9
40	4.03	6.96	78.2	77.1	4.14	6.84	81.6	76.6
42	3.81	6.66	78.2	75.9	3.97	6.50	81.0	74.5
44	3.61	6.37	78.0	74.3	3.81	6.17	80.3	66.0
46	3.43	6.10	77.8	71.5	3.65	5.86	79.7	73.6
48	3.25	5.84	77.6	69.5	3.49	5.57	78.9	75.3
50	3.08	5.59	77.3	72.8	3.35	5.29	78.1	76.1
52	2.92	5.35	77.0	74.1	3.21	5.03	77.0	76.6
54	2.77	5.12	76.7	74.7	3.07	4.78	75.6	76.9
58	2.49	4.69	76.0	75.5	2.82	4.32	70.4	77.3
64	2.12	4.11	74.8	75.9	2.47	3.72	76.4	77.4
70	1.81	3.61	73.0	76.0	2.17	3.20	77.5	77.3
80	1.39	2.90	64.9	75.9	1.75	2.50	78.2	76.8
90	1.07	2.34	71.9	75.5	1.42	1.95	78.2	76.1
100	0.821	1.89	73.0	75.0	1.15	1.52	78.0	75.2
110	0.630	1.52	73.4	74.5	0.927	1.19	77.6	74.2
120	0.484	1.23	73.4	73.9	0.751	0.934	77.1	73.2
130	0.372	0.991	73.3	73.4	0.608	0.731	76.5	72.1
140	0.285	0.800	73.1	72.8	0.493	0.572	75.9	71.0
150	0.219	0.646	72.8	72.2	0.399	0.448	75.2	69.9

Table 2
Time distribution of gaseous concentration (c_y) for C_2H_4 and its adsorption energy (ε) on TiO_2 and Fe_2O_3 solids, before and after γ-irradiation with 8.2 Mrad, at 323.2 K

Time (min)	c_y ($\cdot 10^{-6}$ mol/cm^3)		ε (kJ/mol)		c_y ($\cdot 10^{-6}$ mol/cm^3)		ε (kJ/mol)	
	TiO_2	TiO_2(irrad.)	TiO_2	TiO_2 (irrad.)	Fe_2O_3	Fe_2O_3 (irrad.)	Fe_2O_3	Fe_2O_3 (irrad.)
4	12.0	3.59	83.7	87.4	6.18	6.05	85.9	86.3
6	20.5	5.41	83.5	87.8	9.46	8.76	86.3	87.0
8	25.8	6.48	84.4	89.2	11.4	10.2	87.5	88.8
10	28.9	7.05	86.0	91.5	12.4	10.9	89.6	92.1
12	30.6	7.29	88.5	96.3	12.9	11.1	93.2	101.5
14	31.3	7.33	93.6	100.9	13.0	11.0	109.2	94.3
16	31.4	7.23	96.6	93.0	12.9	10.8	93.7	89.9
18	31.1	7.05	89.5	89.9	12.7	10.5	89.8	87.4
20	30.4	6.82	86.5	87.8	12.4	10.1	87.5	85.7
22	29.6	6.56	84.5	86.3	12.1	9.71	85.9	84.3
24	28.7	6.30	83.0	85.0	11.7	9.30	84.5	83.1
26	27.8	6.02	81.7	83.8	11.3	8.90	83.4	82.1
28	26.8	5.75	80.6	82.7	10.9	8.50	82.3	81.2
30	25.8	5.49	79.6	81.6	10.4	8.11	81.4	80.3
32	24.9	5.23	78.6	80.6	10.1	7.73	80.5	79.5
34	23.9	4.99	77.7	79.4	9.66	7.36	79.6	78.8
36	23.0	4.75	76.8	78.1	9.28	7.02	78.8	78.0
38	22.1	4.53	76.0	76.6	8.92	6.68	78.0	77.3
40	21.2	4.31	75.1	74.4	8.57	6.36	77.3	76.5
42	20.4	4.11	74.3	68.3	8.23	6.06	76.6	75.5
44	19.6	3.91	73.6	72.8	7.90	5.77	75.9	74.4
46	18.8	3.73	72.8	74.5	7.58	5.49	75.2	72.8
48	18.1	3.55	72.2	75.3	7.28	5.23	74.6	69.3
50	17.4	3.38	71.5	75.7	6.99	4.97	74.0	70.0
54	16.0	3.07	70.5	76.2	6.44	4.51	73.1	73.7
58	14.8	2.78	69.7	76.4	5.93	4.09	72.4	75.0
62	13.6	2.53	69.2	76.4	5.46	3.70	71.9	75.7
66	12.5	2.30	68.9	76.4	5.03	3.36	71.7	76.2
70	11.6	2.08	68.7	76.4	4.64	3.05	71.6	76.5
80	9.43	1.64	68.6	76.3	3.78	2.39	71.8	77.0
90	7.69	1.29	68.7	76.2	3.07	1.88	72.1	77.1
100	6.27	1.02	68.7	76.1	2.50	1.47	72.4	77.1
110	5.11	0.801	68.8	75.9	2.03	1.16	72.8	76.9
120	4.17	0.631	68.9	75.8	1.66	0.914	73.1	76.7
130	3.40	0.498	68.9	75.7	1.35	0.720	73.5	76.5
140	2.77	0.392	69.0	75.6	1.09	0.567	73.8	76.2
150	2.26	0.309	69.1	75.5	0.890	0.447	74.2	75.8

series of experimental times, chosen two or more minutes apart one from the other, together with the gaseous concentration of C_2H_4 corresponding to these energy values.

The kinetic physicochemical quantities pertaining to the adsorption phenomenon are given in Table 3, although a functional relation between ε and these quantities would be premature at the present state of knowledge. The energy values of Tables 1 and 2 are based on instantaneous local equilibration of the probe gas C_2H_4 with the solid surface, whilst the kinetic parameters k_1, k_{-1} and k_2 of Table 3 may be connected with the microscopic reversibility equilibrium distribution constant $K=k_1/k_{-1}$. One can calculate from this K value the adsorption energy ε with the help of Eq. 3, i.e., via a considerably different path than that of Eq. 16. The results are given in the last column of Table 3 as ε'. These results are independent of time and do not coincide with the long time values of Tables 1 and 2.

Table 3
Adsorption parameter (k_1), desorption rate constant (k_{-1}), surface reaction rate constant (k_2), detector calibration factor (g) and adsorption energy calculated from $K=k_1/k_{-1}$ (ε') for the interaction of gaseous ethene with four solids (ZnO, PbO, TiO_2, Fe_2O_3), before and after γ-irradiation with 8.2 Mrad, at 323.2 K

Solid	k_1 (s^{-1})	k_{-1} (s^{-1})	k_2 (s^{-1})	g ($\cdot 10^{12}$ cm/mol cm^{-3})	ε' (kJ/mol)
ZnO	$1.20\cdot10^{-3}$	$1.10\cdot10^{-3}$	$2.19\cdot10^{-3}$	1.694	73.6
ZnO(irrad.)	$3.91\cdot10^{-4}$	$2.33\cdot10^{-3}$	$5.28\cdot10^{-3}$	1.458	68.6
PbO	$1.34\cdot10^{-2}$	$9.81\cdot10^{-4}$	$1.46\cdot10^{-4}$	1.462	80.4
PbO(irrad.)	$3.49\cdot10^{-3}$	$3.52\cdot10^{-3}$	$6.31\cdot10^{-4}$	1.438	73.4
TiO_2	$1.02\cdot10^{-2}$	$8.92\cdot10^{-4}$	$2.33\cdot10^{-4}$	1.740	79.9
TiO_2(irrad.)	$2.48\cdot10^{-4}$	$1.83\cdot10^{-3}$	$2.81\cdot10^{-3}$	1.531	68.0
Fe_2O_3	$1.82\cdot10^{-6}$	$3.97\cdot10^{-2}$	$4.44\cdot10^{-2}$	1.561	46.5
Fe_2O_3(irrad.)	$1.13\cdot10^{-5}$	$1.50\cdot10^{-2}$	$1.72\cdot10^{-2}$	1.437	54.1

In Fig. 2 the energy values ε and the adsorbate gaseous concentrations c_y using the solid TiO_2 are plotted as a function of time, adopting 3000 plot points. Analogous plots are obtained with the other solid adsorbents, both, before and after γ-irradiation. The appearance of the functions $c_y=f(t)$ is typical for the so-called *diffusion bands* of the RF-GC method, i.e., increase initially, pass through a maximum and then decline with time. The functions $\varepsilon=h(t)$ usually have a maximum at a time near the time-maximum for the corresponding c_y and then they slowly decrease or level off with time. In the

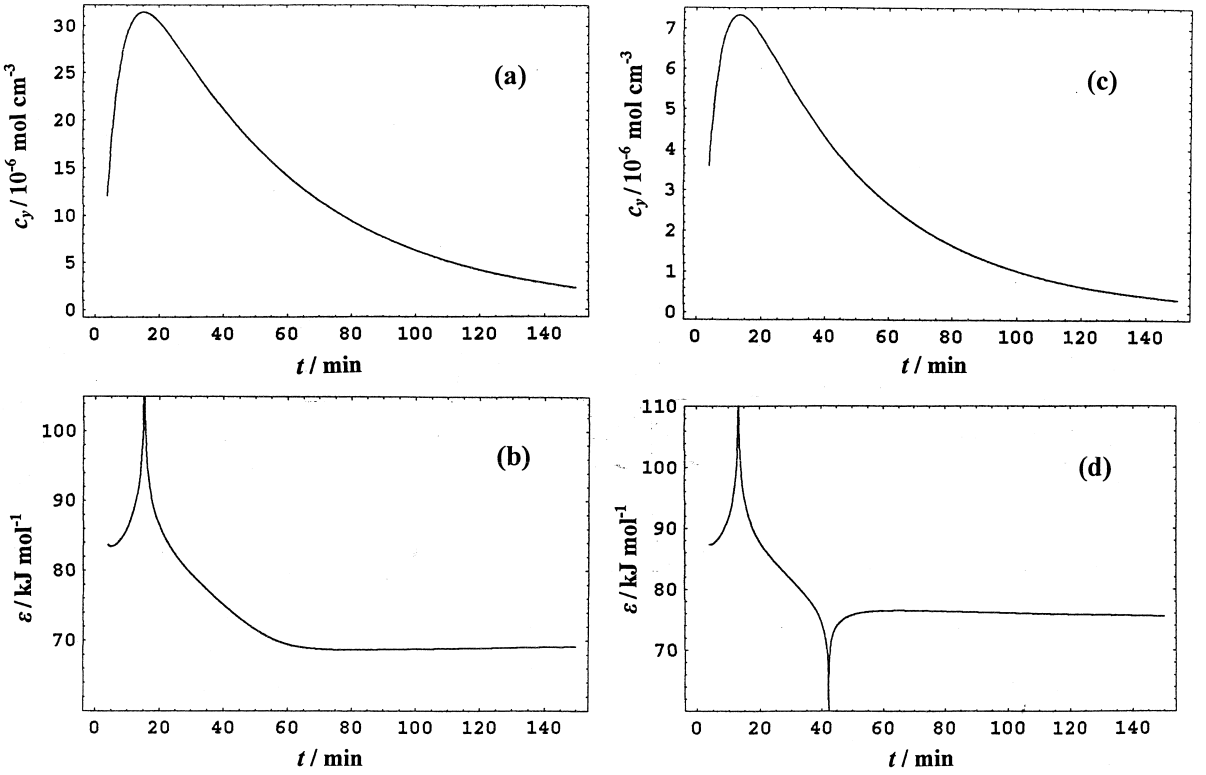

Fig. 2. Plots of gaseous concentrations c_y and adsorption energies ε as a function of the experimental time, at 323.2 K, for the systems C_2H_4/TiO_2 (a, b), and C_2H_4/TiO_2 (irradiated) (c, d), in nitrogen atmosphere.

system C_2H_4/PbO the ε values show a minimum at $t=58$ min. Analogous minima at times $t=42–48$ min appear in all γ-irradiated solids. For PbO (irrad.) the minimum appears at $t=44$ min, i.e., 14 min earlier than the non-irradiated PbO. According to Eqs. 9 and 16, the value of ε experimentally depends on the two partial derivatives $\partial c^*_s/\partial c_y$ and $\partial^2 c^*_s/\partial c_y{}^2$ and, given the experimental form of the function $c_y=f(t)$ (cf. Fig. 2a and c), this explains the discontinuities of ε with time. Physically they mean that at time t the gas molecules are adsorbed exclusively on sites i all of the same energy ε_i. This is not a theoretical assumption to be supported by physical arguments, but a purely experimental fact, as are all plots of Fig. 2. Of course, the above findings call for a theoretical explanation of their physical meaning, but at this premature state of the present method it is difficult to achieve such a goal. The only obvious conclusion is that, owing to the dynamic and changing with time procedure, one observes experimentally transition adsorption energies leading to the final levelling off of their value. Is this due to the creation and destruction of new adsorption sites with time? More experimental results and other additional adsorption properties, like probability density functions with respect to the energies, are required to reach the mechanism of the phenomena. The above additional work is well under way.

The dependence of adsorption energies on time is not a new finding. For example, Kiselev and Yashin [15] report adsorption energies as ''initial'' differential heats of adsorption. Their values in the systems C_2H_4/CaZeolite (53.6 kJ/mol) and C_3H_6/CaZeolite (57.3 kJ/mol) seem comparable to the adsorption energy values given in Tables 1 and 2, ranging between 64.9 and 109.2 kJ/mol. However, this comparison is rather impermissible, since the first refer to global overall values and not to local values as the latter ones. Katsanos et al. [1] found 80.3 kJ/mol for heptane adsorbed on aluminium oxide activated at 440°C. Besides, the above values [15,1] were calculated for a whole temperature range, whilst in the present case all values refer to a single temperature (50°C), considerably lower than before.

One last question is whether our initial adsorption energies, which can be found by extrapolating back to $t=0$ the approximately linear last part of the $\varepsilon=h(t)$ plots (cf. Fig. 2), are more appropriate for comparison with the initial differential heats of adsorption of literature. For example, these extrapolated values for the systems C_2H_4/PbO and C_2H_4/PbO (irrad.) from $t=110$ min and 80 min, respectively, onwards were found 84.3 and 85.1 kJ/mol, respectively. The authors' opinion is in the negative, since the transition time with respect to the energies, as shown in Tables 1 and 2 and Fig. 2b and d, does not permit such an extrapolation. For the present work ''initial adsorption'' is rather a meaningless concept.

Acknowledgements

The generous help of Miss Anna Malliori in the manuscript preparation is warmly acknowledged.

References

[1] N.A. Katsanos, A. Lycourghiotis, A. Tsiatsios, J. Chem. Soc., Faraday Trans. 1 74 (1978) 575.
[2] S.K. Milonjic, M.M. Copecni, Chromatographia 19 (1984) 342.
[3] N.A. Katsanos, R. Thede, F. Roubani-Kalantzopoulou, J. Chromatogr. A 795 (1998) 133.
[4] Ch. Abatzoglou, E. Iliopoulou, N.A. Katsanos, F. Roubani-Kalantzopoulou, A. Kalantzopoulos, J. Chromatogr. A 775 (1997) 211.
[5] D.S. Jovanovic, Colloid Polymer Sci. 235 (1969) 1203, 1214.
[6] M. Heuchel, M. Jaroniec, R.K. Gilpin, J. Chromatogr. 628 (1993) 59.
[7] R.H. Fowler, Statistical Mechanics, 2nd ed, Cambridge University Press, Cambridge, 1936, p. 829.
[8] J.D. Hazlett, C.C. Hsu, B.W. Wojciechowski, J. Chem. Soc., Faraday 2 75 (1979) 602.
[9] W. Rudzinski, B.W. Wojciechowski, J. Coll. Polymer Sci. 255 (1977) 869, 1086.
[10] S. Sircar, J. Coll. Interface Sci. 101 (1984) 452.
[11] M. Jaroniec, S. Sokolowski, A. Waksmundzki, Polish J. Chem. 50 (1976) 779.
[12] W. Rudzinski, D.H. Everett, Adsorption of Gases on Heterogeneous Surfaces, Academic Press, London, 1992, pp. 452–456.
[13] U. Landman, E.W. Montroll, J. Chem. Phys. 64 (1976) 1762.
[14] V. Sotiropoulou, G.P. Vassilev, N.A. Katsanos, H. Metaxa, F. Roubani-Kalantzopoulou, J. Chem. Soc., Faraday Trans. 91 (1995) 485.
[15] A.V. Kiselev, I. Yashin, Gas Adsorption Chromatography, Plenum Press, New York, 1969, p. 47.